Heliyon 10 (2024) e38962

Contents lists available at ScienceDirect

Heliyon

journal homepage: www.cell.com/heliyon

Research article

Suppression of the inflammatory response by oxyresveratrol from the root bark of *Artocarpus lakoocha* Roxb against ultraviolet B-induced keratinocytes mediated by regulating p38 MAPK and AP-1

Kittiya Malaniyom [a], Piyanee Ratanachamnong [b], Poommaree Namchaiw [c,d], Umalee Namdaung [e], Sunit Suksamrarn [f], Yamaratee Jaisin [a,*]

[a] *Department of Pharmacology, Faculty of Medicine, Srinakharinwirot University, Bangkok, 10110, Thailand*
[b] *Department of Pharmacology, Faculty of Science, Mahidol University, Bangkok, 10400, Thailand*
[c] *Neuroscience Center for Research and Innovation, Learning Institute, King Mongkut's University of Technology Thonburi, Bangkok, 10140, Thailand*
[d] *Biological Engineering Program, Faculty of Engineering, King Mongkut's University of Technology Thonburi, Bangkok, 10140, Thailand*
[e] *Herbal and Cannabis Science Program, Faculty of Science and Technology, Bansomdejchaopraya Rajabhat University, Bangkok, 10600, Thailand*
[f] *Department of Chemistry and Center of Excellence for Innovation in Chemistry (PERCH-CIC), Faculty of Science, Srinakharinwirot University, Bangkok, 10110, Thailand*

A B S T R A C T

Oxyresveratrol is a polyphenolic compound present in the root bark of *Artocarpus lakoocha* Roxb. Several studies have reported on its antioxidant, anti-inflammatory, and whitening properties. In this study, we report for the first time that oxyresveratrol alleviates the cytotoxicity of ultraviolet B (UVB) radiation in keratinocytes- . We performed resazurin cell viability, reactive oxygen species (ROS), and Griess assays to investigate the cytoprotective and free radical-scavenging capabilities of oxyresveratrol. The antioxidant effect was demonstrated using the 2,2-diphenyl-1-picryl-hydrazyl (DPPH) free-radical scavenging assay. The inhibition of inflammatory and apoptotic proteins by oxyresveratrol in UVB-irradiated keratinocytes was investigated using western blotting. Pretreated cells with oxyresveratrol exhibited reduced cell death upon UVB exposure, which was mediated by its antioxidant activity. Oxyresveratrol protected cells by inhibiting the mitogen-activated protein kinase p38 and its downstream target, AP-1 transcription factor. These factors led to a decrease in UVB-induced cell inflammation through iNOS and COX-2 expression. Furthermore, the Bax/Bcl-2 ratio was significantly decreased by oxyresveratrol at 10 μM and thus reduced cell apoptosis, as demonstrated by the Hoechst 33342 staining assay. This study revealed the photoprotective effects of oxyresveratrol against UVB\ irradiation in keratinocytes. This strongly supports the benefits of using oxyresveratrol as an ingredient in skincare products for the prevention of sun-damaged skin.

1. Introduction

Extensive exposure to sunlight has harmful effects on human skin [1]. Sunlight is the main source of ultraviolet (UV) radiation, which generally divides into three wavelengths: UVA (λ = 320–400 nm), ultraviolet B (UVB) (λ = 290–320 nm), and UVC (λ = 100–290 nm). UVC radiation is completely absorbed by the ozone layer, whereas UVA and some UVB radiation pass through it [2]. Among all UV radiation sources, continuous exposure to UVB is the major risk factor for skin inflammation and carcinogenesis [3,4]. Moreover, UVB has a direct effect on skin cell inflammation and cell death, whereas UVA is less than 1000 times more damaging than

* Corresponding author.
E-mail address: yamaratee@g.swu.ac.th (Y. Jaisin).

https://doi.org/10.1016/j.heliyon.2024.e38962
Received 27 April 2023; Received in revised form 2 August 2024; Accepted 3 October 2024
Available online 11 October 2024

UVB radiation. A strong correlation exists between UVB-induced skin inflammation and cell death [5–7].

UVB-induced skin inflammation involves the overproduction of reactive oxygen species (ROS) and nitric oxide (NO). Oxidative stress activates the signal transduction of mitogen-activated protein kinase (MAPK) [8,9]. Through a series of phosphorylations, phospho-p38 MAPK activates the transcription factor activator protein-1 (AP-1) [9,10]. Subsequently, the AP-1 transcription factor activates the downstream pathway associated with apoptosis through the Bcl-2 family [11]. In addition to cell death, UVB enhances COX-2 activity, which promotes the conversion of arachidonic acid to prostaglandin E_2 (PGE_2) [12,13] and inducible nitric oxide synthase (iNOS) activity in keratinocytes, which results in the production of pro-inflammatory components [14]. Furthermore, accumulating evidence suggests that the AP-1 transcription factor is the main regulator of keratinocyte viability, proliferation, and differentiation, which ultimately causes skin cancer genesis [15]. The activation of AP-1 is significantly increased in response to UVB exposure in SKH-1 hairless mice [16], which induces its corresponding product, COX-2/PGE_2, and subsequently increases the risk of skin cancer [17]. Therefore, the suppression of the aforementioned key components may be a good target for preventing UVB in sunlight-exaggerated skin phototoxic effects such as cell inflammation and cell death.

For thousands of years, traditional herbal medicines have been used to treat various skin problems and have been integrated as active ingredients in cosmetic products for skin beauty. They are readily available and affordable in several developing countries, including Thailand. The study of the natural compounds presents in traditional herbal medicines and their biological activities is of great interest to the cosmeceutical industry [18]. Because of the abundance of bioactive compounds with anti-inflammatory and antioxidant properties, *Artocarpus lakoocha* Roxb (*A. lakoocha* Roxb) has been intensively studied in recent years. Oxyresveratrol is one of the potent free radical scavengers found in this plant [19]. It is a hydroxyl-substituted stilbene with antineoplastic, neuroprotective, and antioxidant properties [20]. Previous studies have demonstrated that mulberry wood-derived oxyresveratrol exerts anti-inflammatory effects. The lipopolysaccharide (LPS) and interferon-gamma (IFN-γ)-induced nitrite accumulation in microglia cells had been lowered by the pretreatment of oxyresveratrol [21]. In addition, oxyresveratrol and its analogs reduce LPS-induced inflammatory responses in macrophages [22–24]. Oxyresvesveratrol also has an anti-aging potential against UVB irradiation-induced matrix metalloproteinase-1 (MMP-1), mitogen-activated protein kinases (MAPKs), and Protein kinase B (PKB)/The mammalian target of rapamycin (Akt/mTOR) signaling pathways in human fibroblasts [25]. Moreover, it acts as a whitening agent by inhibiting tyrosinase and blocking melanin biosynthesis [26]. Owing to these properties, oxyresveratrol has attracted interest as an ingredient in skincare products. Thereby, oxyresveratrol has been extensively used as a whitening agent in skincare products.

Furthermore, it also protected human epidermal keratinocytes from UVA-induced damage [27]. Although considerable scientific evidence has revealed the biological mechanisms of action of this compound [28], limited studies have explored the anti-inflammatory mechanisms of oxyresveratrol against UVB exposure in keratinocytes. Using a UVB single-exposure keratinocyte cell culture model, we demonstrated the molecular mechanisms of oxyresveratrol photoprotection, with a focus on the underlying mechanism of its anti-inflammatory effect. We found that phospho-p38 and its downstream signaling pathways were suppressed. This study revealed that oxyresveratrol could prevent keratinocyte inflammation and death upon UVB exposure through the inhibition of the AP-1 transcription factor, Bcl-2 family proteins, and pro-inflammatory components, iNOS, COX-2, and PGE_2. Therefore, this study demonstrated the anti-inflammatory capability of oxyresveratrol, which may be useful for fulfilling its pharmacological properties and as an effective ingredient in cosmeceutical products.

2. Materials and methods

2.1. Oxyresveratrol

Oxyresveratrol was provided by Professor Dr. Sunit Suksamrarn, Department of Chemistry, Faculty of Science, Srinakharin Wirot University, Bangkok, Thailand. Oxyresveratrol was isolated from the isolation of oxyresveratrol from the root bark of *A. lakoocha* methanol extract as previously described [29]. A Nuclear Magnetic Resonance (NMR)-based method was used to investigate the NMR spectra of oxyresveratrol, as shown in Supplementary material. The NMR spectrum of oxyresveratrol was confirmed to match that of Likhitwitayawuid, S and Sritularak, B [30]. A stock dilution of oxyresveratrol (200 mM) was liquefied with dimethyl sulfoxide (DMSO). The concentration of DMSO used in media cell culture was finally kept at 0.1 %. The chemical structure of oxyresveratrol was shown in Fig. 1.

2.2. In vitro antioxidant activity

The *in vitro* free radical-scavenging activity of oxyresveratrol was assessed using the 2,2-diphenyl-1-picrylhydrazyl (DPPH) assay

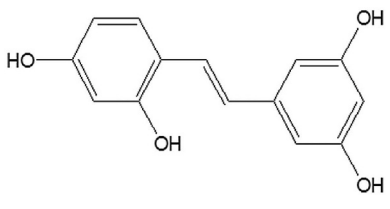

Fig. 1. Chemical structure of oxyresveratrol.

[31]. Twenty microliters of oxyresveratrol as dissolved in 95 % methanol, and then mixed with 180 μL of 0.1 M DPPH solution, followed by incubation in the dark for 15 s. The absorbance was measured using a microplate reader (Bio-Tek Instruments, Winooski, VT, USA) at 515 nm against a blank. Trolox was used as the standard. The percentage DPPH free radical inhibition was calculated using the following equation from our previous study [10].

2.3. Cell culture

HaCaT, a human keratinocyte cell line purchased from Cell Lines Service (Eppelheim, Baden-Württemberg, Germany), is an *in vitro* cell-based model for screening compounds against UVB-induced skin damage and inflammation because it releases several inflammatory mediators, leading to an inflammatory response after UVB exposure [32]. The keratinocytes were cultured in Dulbecco's modified Eagle medium (DMEM) with high glucose mixed with 10 % heat inactivated fetal bovine serum (FBS), 1 % non-essential amino acids, and 0.01 penicillin/streptomycin in a plastic 75 cm^2 cell culture flask at 37 °C in a humidified (>80 %) and 5 % CO_2 incubator (Gibco BRL, Gaithersburg, MD, USA). The cultured cells were soaked in a 0.05 % ethylenediaminetetraacetic acid (EDTA) solution for 5 min, and the adherent cells were detached from the cell culture flask using freshly prepared 0.125 % trypsin-EDTA. The seeded cells were then grown for 24 h before use in subsequent experiments.

2.4. UVB source and treatment

The UV Bio-Link BLX crosslinker (BIO-LINK®, Vilber Lourmat UV-Crosslinker, Deutschland GmbH, Eberhardzell, Germany) sent out UVB radiation from 280 nm to 320 nm, which was used to stimulate cells. Prior to 40 mJ/cm^2 UVB irradiation, the culture media were discarded and the cells were washed with sterile phosphate-buffered saline (PBS) and covered with a thin layer of PBS [9].

2.5. Assessment of cell viability

Viable cells were determined using the cell permeable redox indicator Resazurin Cell Viability Assay Kit (Sigma-Aldrich, St. Louis, MO, USA). Mitochondrial enzymes in viable cells can reduce resazurin (deep blue color) to resorufin products, which show a fluorescence in the culture medium. The intensity of resorufin fluorescence was proportional to the number of viable cells [33]. To determine the cytotoxic effects of oxyresveratrol, keratinocytes were cultured in 96-well cell culture plates at a density of 5×10^4 cells/well. The various concentrations of oxyresveratrol were treated cells for 24 h. To further investigate its cell protective effect, cells that had been seeded on six-well plates were treated with 2.5, 5, and 10 mM of oxyresveratrol for 1 h before exposure to a single UVB irradiation and then left to grow for another 24 h. Then, a 10 % volume of 0.1 % resazurin solution was pipetted into each well, followed by incubation for 3 h in a humidified atmosphere at 37 °C, 5 % CO_2 cell incubator. After incubation, samples were measured using a fluorescent microplate reader (Bio-Tek Instrument, Winooski, Vermont, USA) at 530 nm excitation and 590 nm emission.

2.6. Analyzing cell death by nuclear staining with Hoechst 33342

The cells were seeded in a 35 mm cell culture dish at a density of 2×10^6 cells/dish. After the pretreated cells were maintained under the same experimental conditions as in the previous method, they were incubated in DMEM without phenol red for 24 h. Cells were stained with Hoechst 33342 solution (Invitrogen, Carlsbad, CA, USA) and incubated in the dark for 15 min. The phase contrast of morphological features and fluorescence images of apoptotic nuclei were visualized using a fluorescence microscope (Olympus: DP73 + IX71, IX73P2F, Japan). The ratio of apoptotic to total cells in the dish served as the basis for calculating the apoptotic number.

2.7. Measurement of intracellular ROS

The level of intracellullar ROS in UVB-irradiated keratinocyte cells was evaluated with the fluorescence probe 2′,7′-dichlorodihydrofluorescein diacetate (H_2DCFDA) in accordance with some modification of the manufacturer's protocol. The H_2DCFDA probe was not fluorescent until it penetrated the cell membrane. The enzyme cytoplasmic esterase in living cells cleaves it into a highly fluorescent compound, 2′,7′-dichlorofluorescein (DCF), after reacting with intracellular ROS [34].

Briefly, cells were seeded in 12-well plates at a density of cells 5×10^4 cells/well for 24 h. The cells were preincubated at 2.5, 5, and 10 μM of oxyresveratrol for 1 h, followed by washing the cells with PBS and loading 20 μM of H_2DCFDA dissolved in DMEM without phenol red for 30 min. After that, the cells were washed with 1X PBS, exposed to single UVB irradiation, and incubated in a 37 °C, 5 % CO_2 incubator for 45 min. Additionally, the cells received a single UVB irradiation before 45, 90, and 150 min of incubation and loading with 20 μM of H_2DCFDA. The DCF fluorescence intensity of the cells was immediately measured using a fluorescence microplate reader (Bio-Tek Instruments, Winooski, Vermont, USA) with an excitation wavelength of 485 nm and an emission wavelength of 535 nm. The fluorescence intensity signal was directly proportional to the intracellular ROS levels. H_2O_2 (100 μM) was used as a positive control for UVB-induced intracellular ROS formation.

2.8. Measurement of nitric oxide (NO) production

This assay investigated the effect of UVB-induced increase in NO production in keratinocytes by measuring stable NO metabolites and nitrite content [35]. After seeding cells into six-well plates, the preincubated cells with oxyresveratrol at 2.5, 5, and 10 μM for 1 h

were exposed to single UVB radiation and further incubated in a 37 °C, 5 % CO_2 cell incubator for 24 h. Then, 100 μL of cell culture supernatant was pipetted into a 96-well cell culture plate and concomitantly mixed with sulfanilamide solution (50 μL) and 0.1%NED solution (50 μL). The samples were incubated in the dark for 10 min at room temperature, and the absorbance was measured at 545 and 665 nm within 30 min using a microplate reader (Bio-Tek Instrument, Winooski, Vermont, USA). At 0–100 μm, sodium nitrile diluted in culture media was used for the standard curve. The experimental data were converted to nitrite concentrations based on a standard curve.

2.9. Analysis and evaluation of protein expression

Keratinocytes were seeded onto a 100 mM cell culture dish at a density of 10×10^6 cells/dishs. The preincubated cells with oxyresveratrol at 2.5, 5, and 10 μM for 1 h were exposed to single UVB irradiation, after which the cells were further incubated in a 37 °C, 5 % CO^2 cell incubator for the indicated time. At the end of treatment, the cells were harvested by RIPA buffer mixed with a 1 % protease and phosphatase inhibitor cocktail and further centrifuged at 12,000 rpm for 15 min at 4 °C. The supernatant was collected, and protein concentrations were measured using a Bradford protein assay (Bio-Rad, California, USA). Equal amounts of proteins were subjected to sodium dodecyl-sulfate polyacrylamide gel electrophoresis (SDS-PAGE) and electrophoretically transferred onto nitrocellulose membranes. The nitrocellulose membrane was blocked in a 2 % bovine serum albumin (BSA) solution diluted in tris-bufferes saline with Tween (TBS-T), followed by incubation overnight with the following primary antibodies at 1000-fold dilution in the 2 % BSA solution.

After 24 h, the primary antibodies attached to the membrane were washed thrice with TBS-T for 5 min and subsequently incubated with goat anti-rabbit or goat anti-mouse secondary antibodies (Invitrogen, California, USA) for 1 h at 10,000 dilution in a 2 % BSA solution. The membrane was developed and visualized using an enhanced chemiluminescence (ECL) reagent (EMD Millipore, Darmstadt, Germany). The intensity of each protein band was quantified using ImageJ and normalized to GAPDH (internal control). The primary antibodies used in this study were rabbit polyclonal anti-iNOS (Santa Cruz Biotechnology, Dallas, TX, USA), polyclonal AP-1 and COX-2 (Abcam, Cambridge, UK), polyclonal anti-p-p38, anti-p38, Bax, and BCL-2 (Cell Signaling Technology, Danvers, Massachusetts, USA), and mouse monoclonal anti-GAPDH (Thermo Fisher Scientific, Waltham, Massachusetts, USA).

2.10. The measurement of PGE_2 level

PGE_2 production in cell culture media was measured using a prostaglandin E_2 enzyme-linked immunosorbent assay (ELISA) kit in accordance with the manufacturer's instructions (Cayman Chemical, Michigan, USA). Briefly, cells pre-incubated with oxyresveratrol were exposed to a single UVB irradiation followed by 24 h of cell incubation, and the media were collected and pipetted into an ELISA 96-well precoated plate with goat polyclonal anti-mouse IgG. After that, the samples were added with an anti-PGE_2 monoclonal antibody and acetylcholinesterase linked to PGE_2 (AChE Tracer) followed by incubation at 4 °C, in the dark for 18 h. After incubation, the plate was washed with washing buffer, Ellman's reagent was added, and the plate was incubated in the dark at room temperature for 1 h. Absorbance was immediately measured at wavelengths between 405 and 420 nm using a microplate reader. At 0–1000 pg/mL, PGE_2 diluted in ELISA buffer was used to generate a standard curve. A positive control used in this method was celecoxib, a specific

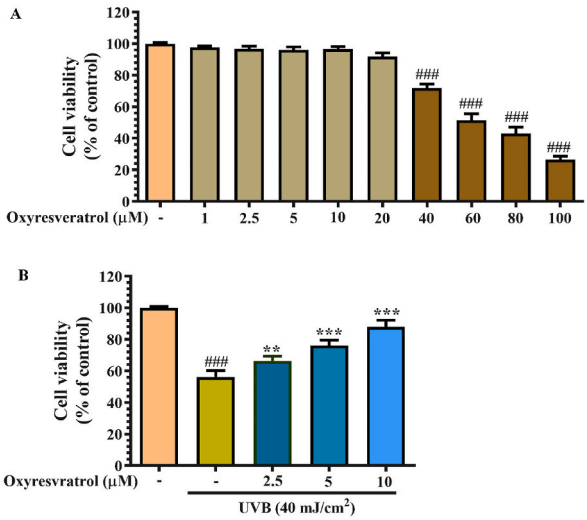

Fig. 2. Effects of various concentrations of oxyresveratrol on cells after 24 h (**A**, n = 8) and the photoprotective effects of oxyresveratrol pretreatment on single UVB irradiation-induced cell toxicity followed by incubation for 24 h (**B,** n = 8). Each cell survival percentage is presented as the mean ± standard error of the mean (SEM) of independent experiments. Mean values among the groups were considered statistically significant at $^{###}p < 0.01$ vs. control group, $^{**}p < 0.01$ and $^{***}p < 0.001$ vs. UVB-irradiated group.

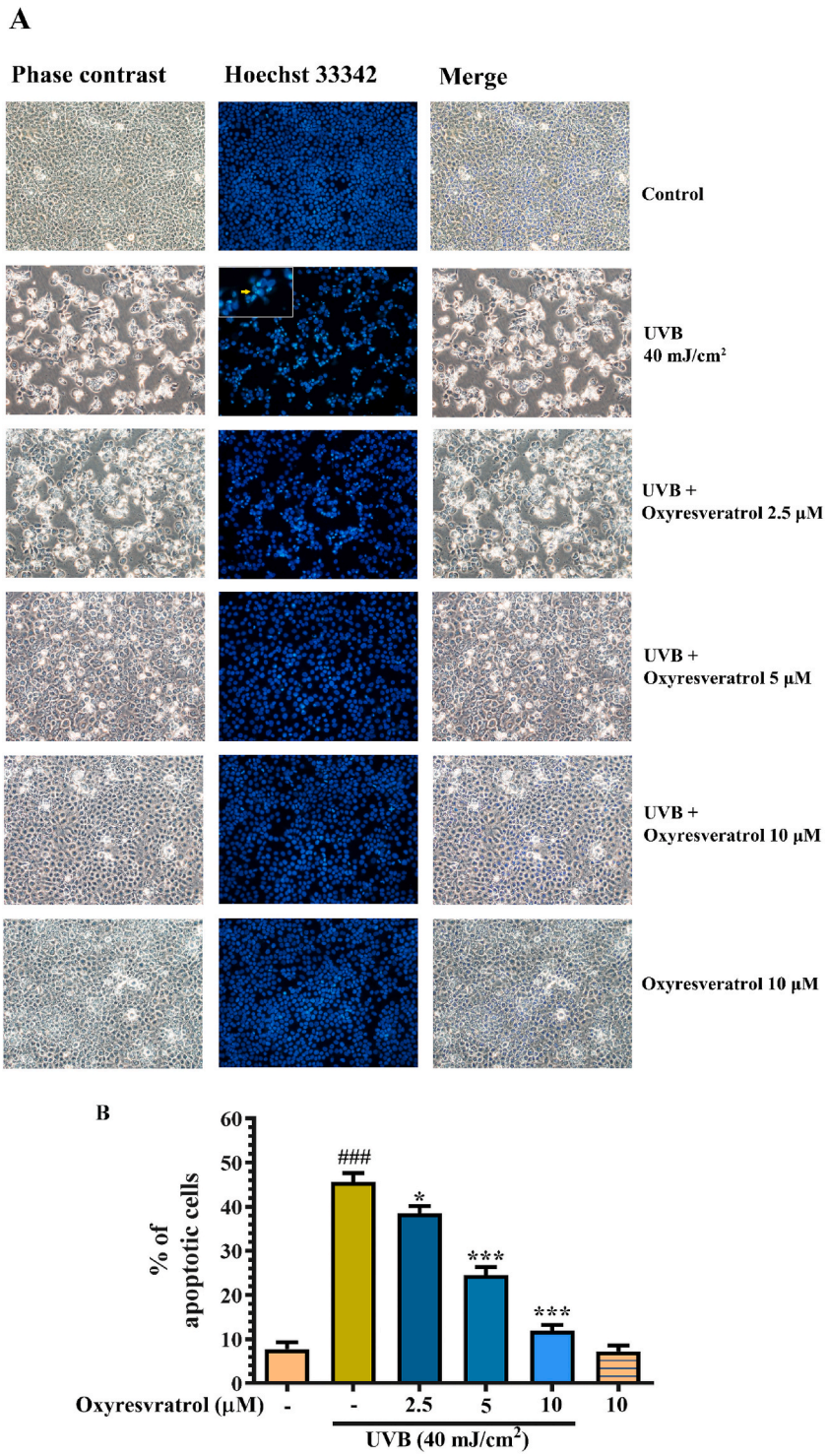

Fig. 3. Effect of oxyresveratrol on single UVB-irradiated keratinocyte cell death. **A** showed cell morphology by phase-contrast microscopy and Hoechst 33342 staining of apoptotic nuclei observed using fluorescence microscopy. Marked apoptotic bodies were observed in the UVB-irradiated cells (inset figure). **B** Representative histogram of the percentage of apoptotic cells counted and averaged from three different areas. Each value is presented as the mean ± SEM of eight independent experiments. Mean values among the groups were considered statistically significant at $^{###}p<0.001$ vs. the control group, $^{*}p<0.05$, $^{***}p<0.001$ vs. the UVB-irradiated group.

COX-2 inhibitor at 10 μM.

2.11. Statistical analysis

Data were analyzed by one-way ANOVA and compared with a Tukey comparison test expressed as the mean ± SEM of six or eight independent experiments. The data was considered statistically significant at a *p*-value equal to 0.05 or lower.

3. Results

3.1. The protective capability of oxyresveratrol against UVB-triggered cell toxicity

The sublethal dose of oxyresveratrol was determined using a resazurin cell viability assay. The concentrations of 1–100 μM of the compound were treated in cell culture for 24 h. Oxyresveratrol showed a non-cytotoxic effect on cells at high concentrations (Fig. 2A). The concentrations of 60 μM and over reduced the cell viability to more than half, whereas those of 10 and lower were barely harmful, with a percentage of viability greater than 96 %. Thus, concentrations of 2.5, 5, and 10 μ M were considered safe and were selected for further analysis.

A single UVB exposure of 40 mJ/cm^2 on cells was used to replicate UVB-induced cytotoxicity. Cell viability was significantly reduced to 56.19 ± 4.0 % compared to the no-UVB radiation control. We demonstrated that the pretreatment of oxyresveratrol at 2.5, 5, and 10 μM for 1 h prior to single UVB exposure significantly recovered cell viability to 66.31 ± 3.07, 76.09 ± 3.45, and 87.82 ± 47.3 %, respectively (Fig. 2B). These results indicated that oxyresveratrol has a photoprotective effect against UVB radiation.

3.2. Anti-apoptosis of oxyresveratrol against UVB-induced keratinocytes

Previous studies have shown that UVB-induced cytotoxicity occurs through apoptosis [36,37]. In this study, we found that a single UVB exposure model could recapitulate cytotoxicity by increasing the apoptotic cell number and appearing as chromatin condensation, as determined by the Hoechst 33342 staining assay. The apoptotic cell evaluation revealed that more than 40 % of cells died from apoptosis upon exposure to single UVB radiation. In addition, phase-contrast imaging revealed morphological changes following UVB exposure at 40 mJ/cm^2. These cells underwent cellular blebbing and shrinkage, which are characteristics of apoptotic cells (Fig. 3A). Pretreatment with oxyresveratrol at 2.5, 5, and 10 μM significantly reduced cell apoptosis upon single UVB exposure by approximately 38, 24, and 11 %, respectively (Fig. 3B). Although the maximum concentration of oxyresveratrol (10 μM) used in this experiment was able to protect cells against UVB radiation, it did not fully recover the cytotoxicity. As shown in Fig. 3B, at 10 μM of oxyresveratrol-pretreated cells had a percentage of cell apoptosis when compared to control cells (Fig. 3B). This explains why UVB radiation is responsible for skin cell death [37].

We further investigated the expression of BCL-2 and BAX (Fig. 4), which play important roles in caspase-dependent apoptosis via the mitochondria. The result showed that UVB irradiation upregulated BAX protein expression and downregulated BCL-2 expression. The ratio of BAX/BCL-2 increased by 2.44 ± 0.29-fold upon single UVB exposure, whereas pretreatment with 2.5, 5, and 10 μM oxyresveratrol significantly decreased the Bax/Bcl-2 ratio by 1.51 ± 0.11-, 1.03 ± 0.07-, and 0.72 ± 0.06-folds, respectively (Fig. 4).

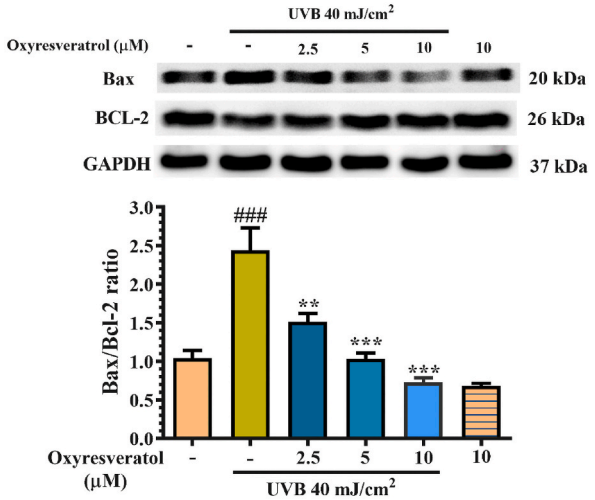

Fig. 4. Effect of oxyresveratrol on BAX/BCL-2 protein expression in single UVB-irradiated cells, followed by incubation for 24 h. Each value is presented as the mean ± SEM of six independent experiments. Mean values among the groups were considered statistically significant at $^{###}p <$ 0.001 vs. control group, $^{**}p <$ 0.01 and $^{***}p <$ 0.001 vs. UVB-irradiated group. (See full and non-adjusted images as files in supplementary material.)

Collectively, these results indicate that UVB-induced apoptosis occurs through BCL-2 family proteins, whereas pretreatment with oxyresveratrol can restore the BAX/BCL-2 ratio, thus reducing UVB-induced cell apoptosis.

3.3. Antioxidant of oxyresveratrol on UVB-irradiated keratinocytes

A single dose of UVB radiation killed cells by activating the BCL-2 family of cell death programs. It could also cause intracellular ROS at the same level as 100 μM H_2O_2 treatment. The secretion of intracellular ROS reached its highest concentration at approximately 45 min after exposure and decreased over time. We found that after the cells were exposed to single UVB irradiation and then incubated for 45, 90, and 150 min, the intracellular ROS levels significantly increased by 1.89 ± 0.054-, 1.57 ± 0.063-, and 1.46 ± 0.099-folds that of the control, respectively (Fig. 5A). The reduction in intracellular ROS levels over time was similar to that of the H_2O_2 treatment, which was used as a positive control. H_2O_2-treated cells were slightly lower in intracellular ROS levels than UVB-irradiated cells, but not statistically different. Therefore, we selected the 45-min incubation time point to determine the photoprotective effect of oxyresveratrol. As shown in Fig. 5B, the preincubation of oxyresveratrol at concentrations of 2.5, 5, and 10 μM significantly reduced the ROS levels by 1.45 ± 0.063-, 1.04 ± 0.047-, and 0.83 ± 0.050-folds of those of the control, respectively, in a dose-dependent manner.

Along with ROS, this study also measured the production of nitric oxide (NO) upon UVB exposure, as determined by the Griess assay. This assay indirectly detects the presence of nitrite, an inert metabolite of NO, in media. The result showed that NO significantly increased to 47.60 ± 3.86 μM upon UVB exposure, whereas it was presented as 2.75 ± 1.14 μM under no UVB radiation. The oxyresveratrol pretreatment at 2.5, 5, and 10 μM exhibited a significant decrease in the nitrile levels to 31.76 ± 4.101, 25.65 ± 1.353, and 19.54 ± 1.691 μM, respectively (Fig. 6). The pretreatment of oxyresveratrol (10 μM) resulted in a significant decrease in NO, although it was not fully restored to the generated NO of the 10 μM treated cell alone ($p < 0.001$). We demonstrated that oxyresveratrol treatment alone did not induce ROS or NO production in keratinocytes. The DPPH assay determined that oxyresveratrol had free radical scavenging activity against DPPH radicals with an IC_{50} of 410.62 μM (Fig. 7B), which is an improvement compared tothe positive control; Trolox with an IC_{50} of 700.23 μM (Fig. 7A). Collectively, this study revealed the antioxidant and anti-inflammatory properties of oxyresveratrol. Thus, it has the potential to reduce skin cell injury caused by sunburn.

3.4. The inhibition effect on protein expression of oxyresveratrol against UVB-irradiated keratinocytes

Previous studies have shown that UVB irradiation induces inflammatory cytokine secretion and inflammation through phosphorylation of p38 MAPK in keratinocytes [9,10,38]. Stimulation of the MAPK signaling pathway initiates the activation of AP-1, which is involved in the upregulation of COX-2 synthesis [9,10,14]. In the present study, we revealed that our single UVB exposure model was capable of inducing p38 MAPK phosphorylation and AP-1 transcription factor by approximately 2-fold compared with no UVB exposure. The pretreatment of oxyresveratrol at 2.5, 5, and 10 μM significantly suppressed the protein expression of phospho-p38 MAPK by 1.75 ± 0.04-, 1.48 ± 0.04-, and 1.28 ± 0.05-folds, respectively (Fig. 8A).

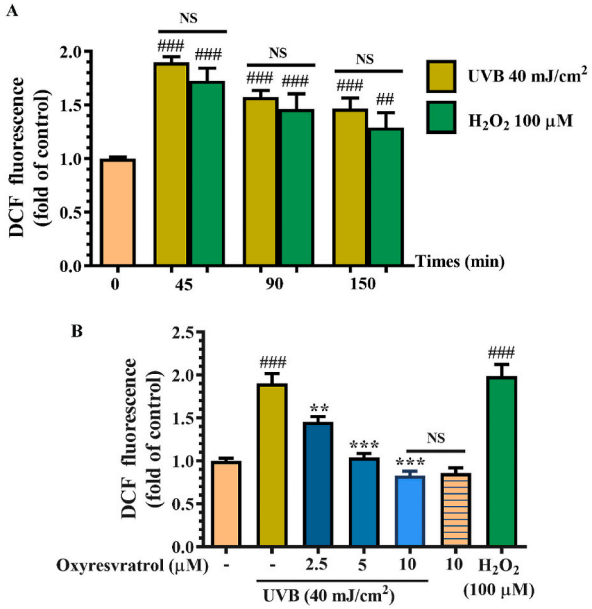

Fig. 5. Time-dependent effect of ROS production (**A**, n = 6) and inhibition of oxyresveratrol against single UVB irradiation-induced ROS production in cells, followed by incubation for 45 min (**B**, n = 6). Each DCF fluorescent intensity value is presented as the mean ± SEM. Mean values among the groups were considered statistically significant at $^{###}p < 0.001$ vs. control group, $^{**}p < 0.01$ and $^{***}p < 0.001$ vs. UVB-irradiated group. NS, non-significant difference between groups.

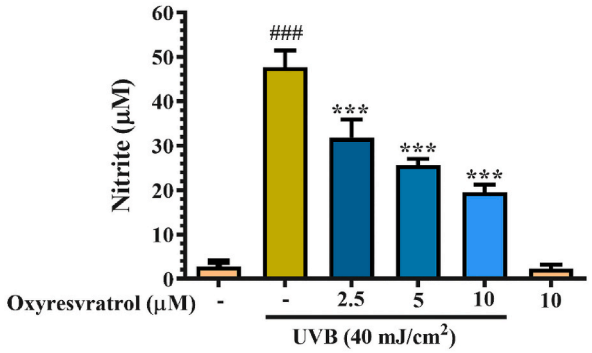

Fig. 6. The inhibitory effect of oxyresveratrol on single UVB irradiation-induced NO production in cells, followed by incubation for 24 h, was assessed using the Griess assay. Each nitrite level value is presented as the mean ± SEM of eight independent experiments. Mean values among the groups were considered statistically significant at $^{###}p < 0.001$ vs. control group, $^{*}p < 0.05$ and $^{***}p < 0.001$ vs. UVB-irradiated group.

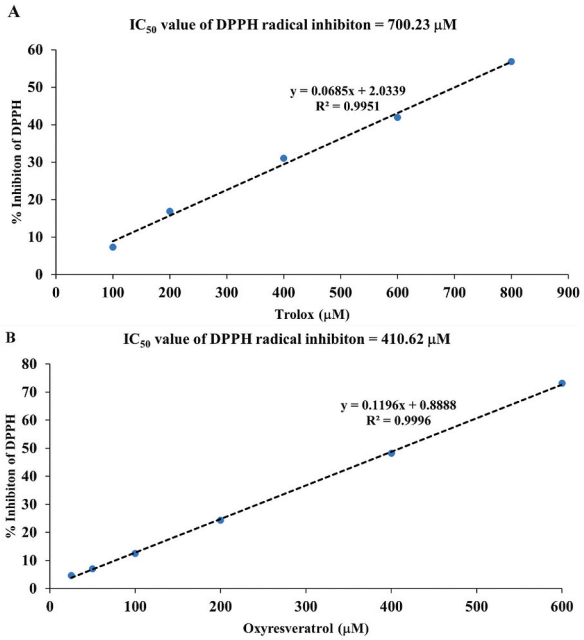

Fig. 7. IC_{50} values of DPPH radical inhibition between oxyresveratrol and Trolox.

In addition, the expression of the AP-1 transcription factor was reduced by 1.01 ± 0.19- and 0.85 ± 0.13-folds following the pretreatment of oxyresveratrol at 5 and 10 μM, respectively, whereas no oxyresveratrol pretreatment showed 0.8-fold reduction compared with no UVB exposure (control cells) (Fig. 8B). The result showed that pretreatment with oxyresveratrol significantly reduced COX-2 protein expression to 1.65 ± 0.06-, 1.42 ± 0.05-, and 1.21 ± 0.05-folds following 2.5, 5, and 10 μM oxyresveratrol pretreatment, respectively, compared with 1.91 ± 0.08-fold reduction with UVB exposure alone (Fig. 8C). The highest concentration of oxyresveratrol treated cells alone did not change the levels of phospho-p38 MAPK, AP-1, or COX-2 compared to the control group. However, adding oxyresveratrol to the cells before a single dose of UVB radiation may lower the upregulation of these signaling proteins. This may subsequently reduce the inflammatory process of skin cells upon UVB exposure.

3.5. The inhibition of iNOS protein expression and PGE_2 production of oxyresveratrol against UVB-irradiated keratinocytes

Along with the activation of the MAPK signaling pathway, UVB exposure subsequently stimulates downstream inflammatory processes, including the iNOS signaling pathway [9,39]. The present study showed that a single UVB irradiation induced iNOS protein expression by 1.90 ± 0.06-fold. The oxyresveratrol pretreatment at 2.5, 5, and 10 μM significantly suppressed iNOS expression by 1.65 ± 0.05-, 1.42 ± 0.06-, and 1.18 ± 0.06-folds, respectively (Fig. 9A). In addition to the increase of iNOS and COX-2 upon UVB exposure, we showed that UVB-irradiation resulted in a significant increase in PGE_2 production, 855.3 ± 5.38 pg/mL, whereas no UVB exposure had 46.96 ± 3.0 pg/mL in keratinocytes. The pretreatment of oxyresveratrol decreased the PGE_2 level to 740.7 ± 30.92, 623.0 ±

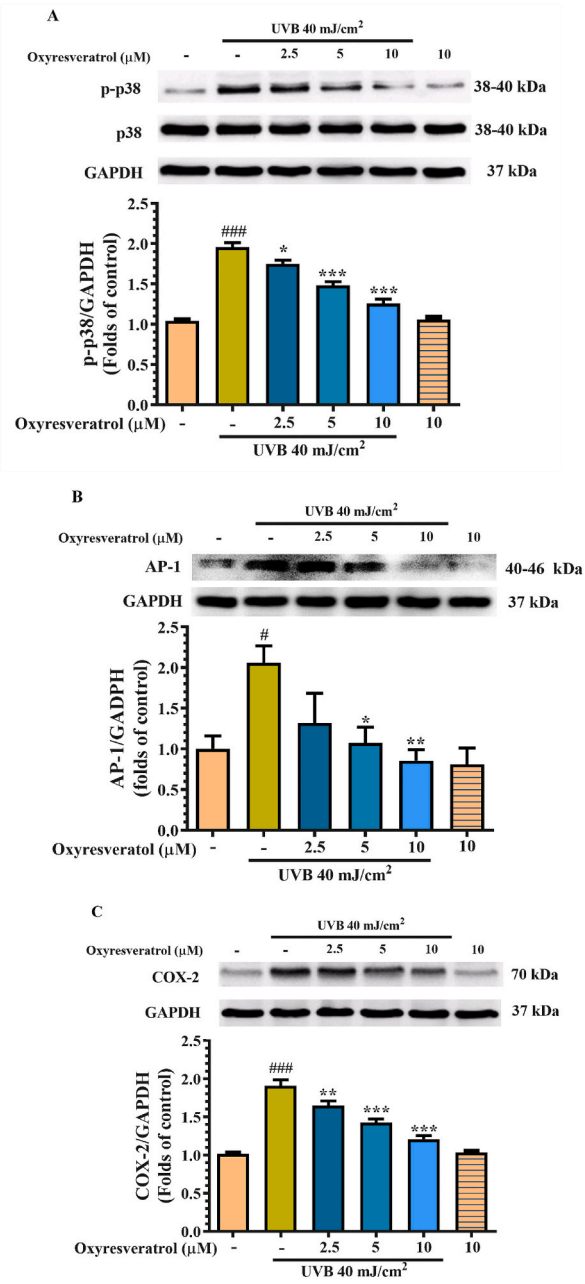

Fig. 8. The effect of oxyresveratrol on p-p38 MAPK (**A**, n = 6), AP-1 (**B**, n = 6), and COX-2 (**C**, n = 8) protein expression in single UVB-irradiated cells was followed by incubation for 6 and 24 h. Each value is presented as means ± SEM. Mean values among the groups were considered statistically significant at $^{\#}p < 0.05$ and $^{\#\#\#}p < 0.001$ vs. control group; $^{*}p < 0.05$, $^{**}p < 0.01$, and $^{***}p < 0.001$ vs. UVB-irradiated group. (See full and non-adjusted images as files in supplementary material.)

43.42, and 271.05 ± 15.40 pg/mL following concentrations of 2.5, 5, and 10 μM, respectively (Fig. 9B).

Based on these results, the anti-inflammatory effects of oxyresveratrol increased with concentration, with 10 μ M oxyresveratrol having the strongest effect. Oxyresveratrol reduced the production of the inflammatory mediator NO in response to UVB irradiation by lowering iNOS expression, and significantly diminished the inflammatory response by suppressing COX-2, p-38 MAPK, and AP-1 protein expression.

4. Discussion and conclusion

UVB radiation exposure is an environmental factor that can cause skin abnormalities. A single exposure to strong UVB radiation or

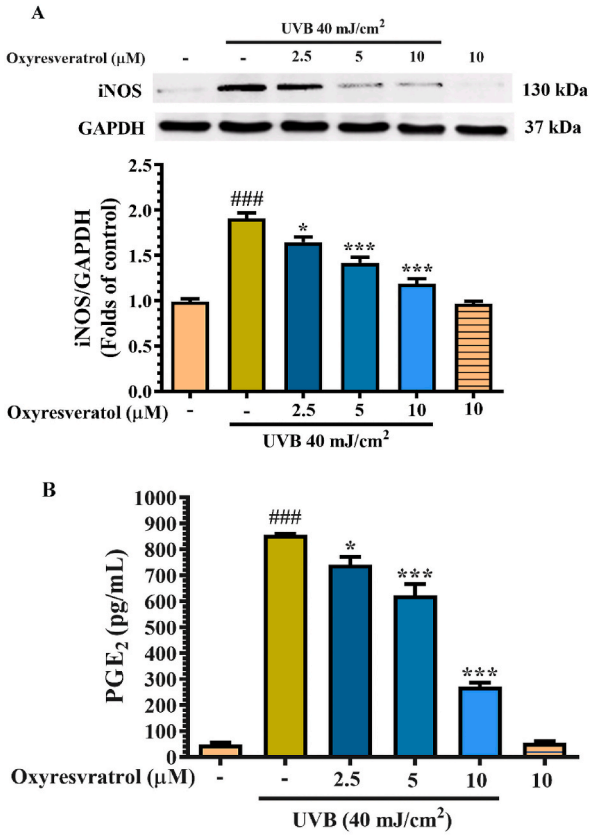

Fig. 9. The effect of oxyresveratrol on the protein expression of iNOS (**A**, n = 8) and PGE_2 (**B**, n = 6) in single UVB-irradiated cells was followed by incubation for 12 and 24 h, respectively. Each value is presented as the mean ± SEM. Mean values among the groups were considered statistically significant at$^{###}p < 0.001$ vs. control group, $^{*}p < 0.05$ and $^{***}p < 0.001$ vs. UVB-irradiated group. (See full and non-adjusted images as files in supplementary material.)

even a low-dose but prolonged exposure results in the generation of ROS and damages the outer layer of the skin. The accumulation of ROS is harmful to DNA and ultimately causes skin cancer [11,17,40]. Keratinocytes are the major cell types in the epidermis. Previous studies revealed that the *in vitro* model of UVB exposure at 30–40 mJ/cm^2 led to cell inflammation and apoptosis in keratinocytes [9], whereas a single exposure to UVB at 70 mJ/cm^2 led to the upregulation of tumor suppressor genes p16 and p53 [41]. Therefore, this cell type has been widely used in cell culture models to study UVB toxicity [32]. The HaCaT keratinocyte cell line is more responsive to UVB exposure than normal keratinocytes [42]. Therefore, we studied the downstream pathways of the inflammatory process following UVB toxicity. The human keratinocyte cell line has a long-lived cell culture expansion that is easily able to release inflammatory mediators in response to oxidative stimuli such as UVB radiation [32]. In this study, we used the HaCaT keratinocyte cell line to study the photoprotective effect of oxyresveratrol, which is related to its anti-inflammatory properties. In traditional Thai medicine, *A. lakoocha* root bark is used as an anthelmintic (oral dose) [43,44]. A recent literature review has summarized the pharmacological properties of *A. lakoocha*, including its antinociceptive, anti-inflammatory, and antioxidant activities [45]. Due to the presence of oxyresveratrol, *A. lakooch*a is widely used in skincare products that promote skin whitening [19]. Oxyresveratrol is a polyphenolic compound found in several plants, especially white mulberry and *Morus alba* L [22]. Oxyresveratrol exerts an inhibitory effect on the expression of melanin by inhibiting tyrosinase activity [26,46]. In addition, it has been reported to possess anti-inflammatory activity and decrease inflammatory mediators in LPS-stimulated macrophages [24].

In addition, oxyresveratrol and its acetylated derivatives reduce metalloproteinase (MMP)-1 expression, which subsequently prevents collagen type I and III degradation in human dermal fibroblasts [25]. Although several studies have reported its ability to combat skin problems, only a limited number of studies have explored the underlying anti-inflammatory mechanism of action that protects cells against UVB-induced HaCaT keratinocyte toxicity. Our results showed that oxyresveratrol from the root bark of *A. lakoocha* exerted cytoprotective effects against UVB exposure. Similar to previous studies, the single UVB exposure model used in the present study showed increased phosphorylation of p38 MAPK, a key activator of COX-2 synthesis [13]. Increased COX-2 levels subsequently increased PGE_2 expression and promoted acute and chronic inflammation, cell proliferation, and skin carcinogenesis [42, 44]. In addition, UVB irradiation induced iNOS activation and increases nitric oxide (NO) levels, which ultimately contributed to destructive cell damage [41]. In the present study, we observed a reduction in phospho-p38 MAPK and AP-1 expression following oxyresveratrol pretreatment. This subsequently reduced the expression of downstream iNOS and COX-2 in the pro-inflammatory

process. As mentioned earlier, AP-1 plays a major role in the regulation of gene expression in response to UVB exposure-induced skin cell inflammation, apoptosis, and potential skin cancer development [16,47]. Oxyresveratrol suppressedAP-1 activation during UVB-induced fibroblast cell aging [25]. However, there is limited scientific evidence demonstrating the inhibitory effect of this compound on UVB-induced p38 MAPK-dependent AP-1 activation in keratinocytes. Therefore, the present study demonstrated that oxyresveratrol negatively regulated both p38 MAPK and AP-1 stimulation in UVB-irradiated keratinocytes, implying its anti-inflammatory capability and possible role in skin cancer prevention. Consistent with our findings, oxyresveratrol was found to reduce inflammation by controlling NF-κB and changing estrogen signaling. It has been suggested that the anti-inflammatory effect of oxyresveratrol occur through the inhibition of ROS and possibly through modulation of the estrogen receptor [48].

Oxyresveratrol reduced ROS/NO levels upon single UVB exposure in a keratinocyte (HaCaT) cell line. The accumulation of ROS/NO resulted in DNA fragmentation and cell death via BCL family proteins, whereas oxyresveratrol recovered cell viability and reduced cell apoptosis, as determined by a reduction in the Bax/Bcl-2 ratio. Mitochondrial dysfunction is the key component of apoptosis. Mitochondrial permeability transitions are important events that lead to UVB-induced apoptosis in keratinocytes [6], and ROS plays a key role in this process [7]. Piceatannol, a metabolite of resveratrol, is a polyphenolic stilbene found in various fruits and has a structure similar to that of oxyresveratrol. According to a report published, piceatannol could reduce intracellular ROS levels in human keratinocytes (HaCaT) after UVB irradiation [49] and recover mitochondrial dysfunction caused by oxidative damage [50]. In line with previous studies, oxyresveratrol, like piceatannol, has four hydroxyl groups in its chemical structure (known as polyhydroxystilbene) (Fig. 1) [29], which exert antioxidant and anti-apoptotic activities, along with diverse therapeutic potentials. Scavenging of DPPH free radicals is the basis for screening compounds with antioxidant activity. As shown in the *in vitro* DPPH assay, oxyresveratrol was a better radical scavenger than the vitamin E derivative Trolox, indicating that oxyresveratrol could act as an H^+ and electron donor. Moreover, excessive intracellular ROS formation due to exposure to UVB radiation significantly contributed to oxidative damage, which harmed skin cells and resulted in cell death. In contrast, the oxyresveratrol pretreatment at 10 μ M was able to reduce intracellular ROS and NO by approximately 43 % and 41 %, respectively, when compared to UVB exposure alone. Collectively, these results suggest that oxyresveratrol possesses good antioxidant effects and can reverse oxidative damage and mitochondrial dysfunction, which are reflected in cell apoptosis. The low concentration of oxyresveratrol at 2.5–10 μM had negligible toxicity to these keratinocyte cells, whereas a higher dose resulted in cell death. Along with its effect on reducing oxidative stress mediated through p38 MAPK inhibition and its downstream activators (AP-1), oxyresveratrol has photoprotective and anti-inflammatory capabilities, which strongly suggests that it is an effective ingredient in cosmeceutical products for alleviating sunburn (inflammation) and possibly preventing skin cancer development.

The human keratinocyte cell line has chromosomal instability and phenotypic variation compared to the donor tissue, but it has numerous benefits, such as being easy to culture and handle and providing an endless supply of material. The HaCaT cell line has some limitations in studying the cell proliferation rate of the psoriatic model triggered by the cytokines TNF-α, IFN-γ, and IL-17 [51]. Although cultured primary human keratinocytes closely represent their origin, their limited life span, difficulty in handling, more time for cell growth, and the requirement of a specifically optimized medium can restrict the use of these cells [52]. Therefore, our 2D keratinocyte (HaCaT) model was appropriate for studying the molecular mechanisms of oxyresveratrol in ultraviolet radiation-induced cell inflammation and toxicity. To overcome these limitations, future studies need to be performed in animal and human models to improve our understanding of the therapeutic efficacy and safety of the topical application of oxyresveratrol in inflammatory skin models. All together, these findings strongly support the pharmacological potential of oxyresveratrol underlying its mechanism of action against ultraviolet radiation-triggered keratinocyte inflammatory responses and cell damage.

CRediT authorship contribution statement

Kittiya Malaniyom: Investigation, Data curation, Formal analysis. **Piyanee Ratanachamnong:** Writing – review & editing, Writing – original draft, Methodology, Investigation, Data curation. **Poommaree Namchaiw:** Writing – review & editing, Writing – original draft. **Umalee Namdaung:** Validation, Resources. **Sunit Suksamrarn:** Resources, Validation. **Yamaratee Jaisin:** Writing – review & editing, Writing – original draft, Supervision, Project administration, Methodology, Conceptualization.

Data availability

Data supporting the findings of this study are available upon reasonable request.

Additional information

As all data and results are presented herein, no additional information is available for this paper.

Funding

This research was funded by a research grant (no.141/2561) from the Faculty of Medicine, Srinakharinwirot University, Thailand.

Declaration of competing interest

The authors declare that they have no known competing financial interests or personal relationships that could have appeared to

influence the work reported in this paper.

Acknowledgements

The authors thank the Department of Pharmacology, Faculty of Medicine, and Strategic Wisdom and Research Institute, Srinakharinwirot University, Thailand, for their research support. We also express our gratitude for the support of Sunit Suksamrarn, the Center of Excellence for Innovation in Chemistry (PERCH-CIC), and the Commission on Higher Education.

Appendix A. Supplementary data

Supplementary data to this article can be found online at https://doi.org/10.1016/j.heliyon.2024.e38962.

References

[1] Wilson B. Dale, S. Moon, F. Armstrong, Comprehensive review of ultraviolet radiation and the current status on sunscreens, The Journal of clinical and aesthetic dermatology 5 (9) (2012) 18–23.
[2] E. Dupont, J. Gomez, D. Bilodeau, Beyond UV radiation: a skin under challenge, Int. J. Cosmet. Sci. 35 (3) (2013) 224–232.
[3] R. Prasad, S.K. Katiyar, Prostaglandin E2 Promotes UV radiation-induced immune suppression through DNA hypermethylation, Neoplasia 15 (7) (2013) 795–804.
[4] S.E. Dickinson, E.R. Olson, J. Zhang, S.J. Cooper, T. Melton, P.J. Criswell, et al., p38 MAP kinase plays a functional role in UVB-induced mouse skin carcinogenesis, Mol. Carcinog. 50 (6) (2011) 469–478.
[5] M. Ciążyńska, I. Olejniczak-Staruch, D. Sobolewska-Sztychny, J. Narbutt, M. Skibińska, A. Lesiak, Ultraviolet radiation and chronic inflammation—molecules and mechanisms involved in skin carcinogenesis: a narrative review, Life 326 (11) (2021) 1–14.
[6] S.J. Lee, J.W. Park, Enhancement of UVB radiation-mediated apoptosis by knockdown of cytosolic NADP+-dependent isocitrate dehydrogenase in HaCaT cells, BMB Rep 47 (4) (2014) 209–214.
[7] H.C. Ryu, C. Kim, J.Y. Kim, J.H. Chung, J.H. Kim, UVB radiation induces apoptosis in keratinocytes by activating a pathway linked to "BLT2-reactive oxygen species", J. Invest. Dermatol. 130 (4) (2010) 1095–1106.
[8] S.D. Sharma, S.M. Meeran, S.K. Katiyar, Dietary grape seed proanthocyanidins inhibit UVB-induced oxidative stress and activation of mitogen-activated protein kinases and nuclear factor-κB signaling in *in vivo* SKH-1 hairless mice, Mol. Cancer Therapeut. 6 (3) (2007) 995–1005.
[9] Y. Jaisin, P. Ratanachamnong, O. Wongsawatkul, A. Watthammawut, K. Malaniyom, S. Natewong, Antioxidant and anti-inflammatory effects of piperine on UV-B-irradiated human HaCaT keratinocyte cells, Life Sci. 263 (2020) 1–9.
[10] S. Natewong, C. Niwaspragrit, P. Ratanachamnong, P. Samatiwat, P. Namchaiw, Y. Jaisin, Photo-protective and anti-inflammatory effects of Antidesma thwaitesianum Müll. Arg, fruit extract against UVB-induced keratinocyte cell damage. Molecules 27 (15) (2022) 1–15.
[11] H.C. Ryu, C. Kim, J.Y. Kim, J.H. Chung, J.H. Kim, UVB radiation induces apoptosis in keratinocytes by activating a pathway linked to "BLT2-reactive oxygen species", J. Invest. Dermatol. 130 (4) (2010) 1095–1106.
[12] W. Chen, Q. Tang, M.S. Gonzales, G.T. Bowden, Role of p38 MAP kinases and ERK in mediating ultraviolet-B induced cyclooxygenase-2 gene expression in human keratinocytes, Oncogene 20 (2001) 3921–3926.
[13] N.S. Fernau, D. Fugmann, M. Leyendecker, K. Reimann, S. Grether-Beck, S. Galban, et al., Role of HuR and p38MAPK in ultraviolet B-induced post-transcriptional regulation of COX-2 expression in the human keratinocyte cell line HaCaT, J. Biol. Chem. 285 (6) (2010) 3896–3904.
[14] K.S. Choi, J.K. Kundu, K.S. Chun, H.K. Na, Y.J. Surh, Rutin inhibits UVB radiation-induced expression of COX-2 and iNOS in hairless mouse skin: p38 MAP kinase and JNK as potential targets, Arch. Biochem. Biophys. 559 (2014) 38–45.
[15] R.L. Eckert, G. Adhikary, C.A. Young, R. Jans, J.F. Crish, W. Xu, et al., AP1 transcription factors in epidermal differentiation and skin cancer, Journal of Skin Cancer 2013 (2013) 1–9.
[16] S.J. Cooper, J. MacGowan, J. Ranger-Moore, M.R. Young, N.H. Colburn, G.T. Bowden, Expression of dominant negative c-jun inhibits ultraviolet B-induced squamous cell carcinoma number and size in an SKH-1 hairless mouse model, Mol. Cancer Res. 1 (11) (2003) 848–854.
[17] C.S. Tripp, E.A.G. Blomme, K.S. Chinn, M.M. Hardy, P. LaCelle, A.P. Pentland, Epidermal COX-2 induction following ultraviolet irradiation: suggested mechanism for the role of COX-2 inhibition in photoprotection, J. Invest. Dermatol. 121 (4) (2003) 853–861.
[18] H.M. Ekiert, A. Szopa, Biological activities of natural products, Molecules 25 (23) (2020) 1–7.
[19] S. Maneechai, K. Likhitwitayawuid, B. Sritularak, C. Palanuvej, N. Ruangrungsi, P. Sirisa-ard, Quantitative analysis of oxyresveratrol content in *Artocarpus lakoocha* and 'Puag-Haad', Med. Princ. Pract. 18 (3) (2009) 223–227.
[20] U.B. Jagtap, V.A. Bapat, Artocarpus: a review of its traditional uses, phytochemistry and pharmacology, J. Ethnopharmacol. 129 (2) (2010) 142–166.
[21] P. Lorenz, S. Roychowdhury, M. Engelmann, G. Wolf, T.F.W. Horn, Oxyresveratrol and resveratrol are potent antioxidants and free radical scavengers: effect on nitrosative and oxidative stress derived from microglial cells, Nitric Oxide 9 (2) (2003) 64–76.
[22] K.-O. Chung, B.-Y. Kim, M.-H. Lee, Y.-R. Kim, H.-Y. Chung, J.-H. Park, et al., In-vitro and in-vivo anti-inflammatory effect of oxyresveratrol from Morus alba L, J. Pharm. Pharmacol. 55 (12) (2003) 1695–1700.
[23] H.S. Lee, D.H. Kim, J.E. Hong, J.Y. Lee, E.J. Kim, Oxyresveratrol suppresses lipopolysaccharide-induced inflammatory responses in murine macrophages, Hum. Exp. Toxicol. 34 (8) (2014) 808–818.
[24] W. Thaweesest, V. Buranasudja, R. Phumsuay, C. Muangnoi, O. Vajragupta, B. Sritularak, et al., Anti-inflammatory activity of oxyresveratrol tetraacetate, an Ester prodrug of oxyresveratrol, on lipopolysaccharide-stimulated RAW264.7 macrophage cells, Molecules 27 (12) (2022) 1–17.
[25] J.E. Lee, J. Oh, D. Song, M. Lee, D. Hahn, Y.C. Boo, et al., Acetylated resveratrol and oxyresveratrol suppress UVB-induced MMP-1 expression in human dermal fibroblasts, Antioxidants 10 (8) (2021) 1–18.
[26] P. Tengamnuay, K. Pengrungruangwong, I. Pheansri, K. Likhitwitayawuid, Artocarpus lakoocha heartwood extract as a novel cosmetic ingredient: evaluation of the in vitro anti-tyrosinase and in vivo skin whitening activities, Int. J. Cosmet. Sci. 28 (4) (2006) 269–276.
[27] S. Hu, F. Chen, M. Wang, Photoprotective effects of oxyresveratrol and Kuwanon O on DNA damage induced by UVA in human epidermal keratinocytes, Chem. Res. Toxicol. 28 (3) (2015) 541–548.
[28] K. Likhitwitayawuid, Oxyresveratrol: sources, productions, biological activities, pharmacokinetics, and delivery systems, Molecules 26 (14) (2021) 1–30.
[29] U. Namdaung, A. Athipornchai, T. Khammee, M. Kuno, S. Suksamrarn, 2-Arylbenzofurans from Artocarpus lakoocha and methyl ether analogs with potent cholinesterase inhibitory activity, Eur. J. Med. Chem. 143 (2018) 1301–1311.
[30] K. Likhitwitayawuid, B. Sritularak, A new dimeric stilbene with tyrosinase inhibitiory activity from Artocarpus gomezianus, Journal of Natural Products 64 (11) (2001) 1457–1459.
[31] T. Shimamura, Y. Sumikura, T. Yamazaki, A. Tada, T. Kashiwagi, H. Ishikawa, et al., Applicability of the DPPH assay for evaluating the antioxidant capacity of food additives, Inter-laboratory evaluation study &ndash. Analytical Sciences 30 (7) (2014), 717-21.

[32] I. Colombo, E. Sangiovanni, R. Maggio, C. Mattozzi, S. Zava, Y. Corbett, et al., HaCaT cells as a reliable in vitro differentiation model to dissect the inflammatory/Repair response of human keratinocytes, Mediat. Inflamm. 2017 (2017) 1–12.
[33] J. O'Brien, I. Wilson, T. Orton, F. Pognan, Investigation of the Alamar Blue (resazurin) fluorescent dye for the assessment of mammalian cell cytotoxicity, Eur. J. Biochem. 267 (17) (2000) 5421–5426.
[34] A. Gomes, E. Fernandes, J.L.F.C. Lima, Fluorescence probes used for detection of reactive oxygen species, J. Biochem. Biophys. Methods 65 (2) (2005) 45–80.
[35] D. Giustarini, R. Rossi, A. Milzani, I. Dalle-Donne, Nitrite and nitrate measurement by Griess reagent in human plasma: evaluation of interferences and standardization, in: Methods in Enzymology, vol. 440, Academic Press, 2008, pp. 361–380.
[36] A.-S. Gary, P.J. Rochette, Apoptosis, the only cell death pathway that can be measured in human diploid dermal fibroblasts following lethal UVB irradiation, Sci. Rep. 10 (1) (2020) 1–11.
[37] C. Khalil, W. Shebaby, UVB damage onset and progression 24h post exposure in human-derived skin cells, Toxicol Rep 4 (2017) 441–449.
[38] A.L. Kim, J.M. Labasi, Y. Zhu, X. Tang, K. McClure, C.A. Gabel, et al., Role of p38 MAPK in UVB-induced inflammatory responses in the skin of SKH-1 hairless mice, J. Invest. Dermatol. 124 (6) (2005) 1318–1325.
[39] E.J. Chang, J.K. Kundu, L. Liu, J.W. Shin, Y.J. Surh, Ultraviolet B radiation activates NF-κB and induces iNOS expression in HR-1 hairless mouse skin: role of IκB kinase-β, Mol. Carcinog. 50 (4) (2011) 310–317.
[40] S. Wu, L. Wang, A.M. Jacoby, K. Jasinski, R. Kubant, T. Malinski, Ultraviolet B light-induced nitric oxide/peroxynitrite imbalance in keratinocytes–implications for apoptosis and necrosis, Photochem. Photobiol. 86 (2) (2010) 389–396.
[41] Z.Y. Abd Elmageed, R.L. Gaur, M. Williams, M.E. Abdraboh, P.N. Rao, M.H. Raj, et al., Characterization of coordinated immediate responses by p16INK4A and p53 pathways in UVB-irradiated human skin cells, J. Invest. Dermatol. 129 (1) (2009) 175–183.
[42] V. Muthusamy, T.J. Piva, A comparative study of UV-induced cell signalling pathways in human keratinocyte-derived cell lines, Arch. Dermatol. Res. 305 (9) (2013) 817–833.
[43] N. Saowakon, T. Tansatit, C. Wanichanon, W. Chanakul, V. Reutrakul, P. Sobhon, Fasciola gigantica: anthelmintic effect of the aqueous extract of Artocarpus lakoocha, Exp. Parasitol. 122 (4) (2009) 289–298.
[44] P. Charoenlarp, P. Radomyos, D. Bunnag, The optimum dose of Puag-Haad in the treatment of taeniasis, J. Med. Assoc. Thail. 72 (2) (1989) 71–73.
[45] P. Sitorus, J.M. Keliat, V. Asfianti, M. Muhammad, D. Satria, A literature review of Artocarpus lacucha focusing on the phytochemical constituents and pharmacological properties of the plant, Molecules 27 (20) (2022) 1–15.
[46] K.-T. Park, J.-K. Kim, D. Hwang, Y. Yoo, Y.-H. Lim, Inhibitory effect of mulberroside A and its derivatives on melanogenesis induced by ultraviolet B irradiation, Food Chem. Toxicol. 49 (12) (2011) 3038–3045.
[47] S.J. Cooper, G.T. Bowden, Ultraviolet B regulation of transcription factor families: roles of nuclear factor-kappa B (NF-kappaB) and activator protein-1 (AP-1) in UVB-induced skin carcinogenesis, Curr. Cancer Drug Targets 7 (4) (2007) 325–334.
[48] J. Wei, J.R. Chen, E.M.A. Pais, T.Y. Wang, L. Miao, L. Li, et al., Oxyresveratrol is a phytoestrogen exerting anti-inflammatory effects through NF-κB and estrogen receptor signaling, Inflammation 40 (4) (2017) 1285–1296.
[49] H. Maruki-Uchida, I. Kurita, K. Sugiyama, M. Sai, K. Maeda, T. Ito, The protective effects of piceatannol from passion fruit (*Passiflora edulis*) seeds in UVB-irradiated keratinocytes, Biol. Pharm. Bull. 36 (5) (2013) 845–849.
[50] J. Liu, P. Mai, Z. Yang, Z. Wang, W. Yang, Z. Wang, Piceatannol protects PC-12 cells against oxidative damage and mitochondrial dysfunction by inhibiting autophagy via SIRT3 pathway, Nutrients 15 (13) (2023) 1–13.
[51] A.G. Soboleva, A.D. Zolotarenko, V.V. Sobolev, S.A. Bruskin, E.S. Piruzian, A.V. Mezentsev, [Genetically predetermined limitation in the use of HaCaT cells that affects their ability to serve as an experimental model of psoriasis], Genetika 50 (10) (2014) 1222–1231.
[52] J.P.H. Smits, H. Niehues, G. Rikken, I. van Vlijmen-Willems, G. van de Zande, P. Zeeuwen, et al., Immortalized N/TERT keratinocytes as an alternative cell source in 3D human epidermal models, Sci. Rep. 7 (1) (2017) 1–14.